International Journal of Thermo-Fluid Systems and Sustainable Energy
http://dx.doi.org/10.62762/IJTSSE.2026.808760

RESEARCH ARTICLE

Modeling And Simulation Of Oil Film Influence On Hydraulic Piston Pump Vibrations

Avae Berger[1,*], **Jiming Ma**[1], **Yunrui Zhang**[1] and **Xiangxiang Tian**[1]

[1] Sino-French Engineer School (École Centrale de Pékin), Beihang University (BUAA), Beijing 100191, China

Abstract

This paper presents a coupled numerical-analytical framework for investigating the influence of the oil film dynamics on the vibration characteristics of the hydraulic piston pump. A finite difference solver is developed to compute the hydrodynamic pressure distribution in the distribution plate under realistic operating conditions, from which equivalent stiffness and damping coefficients are extracted using analytical squeeze-film relations and integrated into a single-degree-of-freedom vibration model. For the baseline case ($\mu = 7.7 \times 10^{-4}$ Pa·s, $\omega = 4000$ rpm, $p_p = 21.5$ MPa, $\gamma = 14°$), the simulation yields a mean pressure of 4.72 MPa and a stable mean oil film thickness of 5.70×10^{-4} m, resulting in a calibrated stiffness of 1.97×10^{7} N·m^{-1} and a damping coefficient of 3.21×10^{-4} N·s·m^{-1}. Two coefficient extraction methods are compared; although they reveal consistent trends across operating conditions, they differ by several orders of magnitude, highlighting the sensitivity of dynamic coefficient estimation to modeling assumptions. The vibration analysis yields a natural frequency of approximately 6.56 kHz and a near-zero damping ratio across all operating conditions investigated. These results demonstrate that while the oil film provides substantial elastic support, its intrinsic damping capacity is insufficient for passive vibration suppression, underscoring the necessity of additional structural or fluid-borne damping mechanisms in the design of low-vibration hydraulic pumps.

Keywords: oil film, piston pump, dynamic coefficients, vibrations.

1 Introduction

Rotating machines are at the heart of modern industry and energy systems, where operational reliability and efficiency often depend on the control of friction, wear, and vibration phenomena. Within this category, fluid power pumps and motors are essential components in aerospace, automotive, and heavy machinery applications, ensuring power transmission through pressurized fluids [1, 2, 14]. Among these, hydraulic piston pumps are particularly valued for their high-pressure capability. Compared with gear or vane pumps, axial piston pumps offer superior performance and are therefore widely adopted in demanding environments [1, 2]. Their reliability is crucial because unexpected vibrations can lead to

Submitted: 09 March 2026
Accepted: 27 April 2026
Published: 04 June 2026

Vol. 2, **No.** 2, 2026.
10.62762/IJTSSE.2026.808760

***Corresponding author:**
Avae Berger
avae.berger@centralepekin.cn

Citation
Berger, A., Ma, J., Zhang, Y., & Tian, X. (2026). Modeling And Simulation Of Oil Film Influence On Hydraulic Piston Pump Vibrations. *International Journal of Thermo-Fluid Systems and Sustainable Energy*, 2(2), 51–62.

wear, energy losses, and catastrophic failure [3, 4]. The tribological interface between piston and cylinder, separated by a thin lubricating oil film, plays a central role [5–7]. This oil film simultaneously supports loads, damps vibrations, and prevents metal-to-metal contact. Beyond reducing friction and wear, a proper lubricant film dissipates the heat generated at the contact interface, protects surfaces against corrosion, and prevents seizure during operation. The performance of this film directly influences energy efficiency, vibration stability, and the overall service life of the pump.

The broader context of carbon neutrality further motivates the present study. Hydraulic piston pumps are widely deployed in industrial, aerospace, and heavy machinery systems that collectively account for a significant share of global energy consumption. Mechanical losses arising from friction, wear, and vibration at lubricated interfaces directly translate into energy inefficiency and elevated carbon emissions over the operational lifetime of these machines. Reducing vibration-induced losses through improved understanding of oil film dynamics therefore contributes, at least indirectly, to the objectives of energy transition and decarbonization. Furthermore, the trend toward electrification and hydrogen-based power systems in aerospace and industrial applications places new demands on hydraulic components in terms of compactness, reliability, and energy efficiency, all of which are influenced by lubrication quality. By establishing a physically consistent model of oil film stiffness and damping in hydraulic piston pumps, this work provides a foundation for the design of more efficient, lower-loss hydraulic systems aligned with carbon neutrality goals.

The lubrication behavior and vibration response of hydraulic piston pumps have been extensively studied using classical fluid power theory and hydrodynamic lubrication models [1, 2, 8]. More recent studies have further highlighted the importance of oil-film stiffness and damping in governing the dynamic response and stability of lubricated interfaces, particularly under oscillatory loading conditions [9, 10]. These works confirm that lubrication-induced dynamic coefficients play a decisive role in the vibration behaviour of piston pumps and motivate the development of coupled lubrication–vibration modeling approaches.

Modeling of lubrication phenomena in hydraulic components is commonly based on the Reynolds equation, which describes the pressure distribution within thin fluid films and forms the theoretical foundation of hydrodynamic lubrication analysis. Various numerical strategies, including finite difference and finite element methods, have been developed to solve this equation for complex geometries and transient operating conditions [11]. Beyond classical numerical approaches, analytical and semi-analytical methods such as the homotopy perturbation method [14] and effective series solution techniques have also been applied to boundary value problems arising in fluid mechanics and heat transfer, offering convergent closed-form approximations for nonlinear differential equations. Beyond pressure field computation, thermal effects and elastic deformation at lubricated interfaces introduce additional complexity; thermal elastohydrodynamic analyses of the piston–cylinder interface have demonstrated that heat transfer and surface compliance significantly affect film thickness evolution and load distribution in axial piston machines [12]. These studies primarily focus on pressure fields, load-carrying capacity, and film thickness evolution under different pump configurations.

In parallel, extensive research has examined the dynamic and vibration behaviour of axial piston pumps under coupled mechanical-hydraulic excitation. Several investigations have analyzed how operating conditions, pressure pulsations, and fluid-structure interactions affect the overall vibration response and noise generation of these machines [3–5, 16–18]. In aerospace hydraulic systems, pipeline vibration and pressure pulsation represent particularly critical concerns, and comprehensive reviews of vibration analysis and control strategies for aircraft hydraulic pipeline systems have documented the state of the art in this domain [15]. Multibody dynamic formulations and numerical simulations have been applied to predict excitation mechanisms related to the swash-plate motion, piston reciprocation, and hydrodynamic pressure variations within the film [1, 2, 7]. Beyond pressure and kinematic analyses, lubrication theory also provides a dynamic description of the oil film response under oscillatory loading. Classical lubrication theory provides well-established analytical formulations for oil-film pressure, stiffness, and damping, which have been widely applied to hydraulic piston pumps and lubricated interfaces [2, 8, 10]. The tribodynamic coupling between the lubricating film and structural vibration has also been studied through elastohydrodynamic lubrication theory. Foundational models have described the elastic and viscous response of the oil film within hydraulic pumps, defining the equivalent stiffness and damping behaviour of the lubricated interfaces [1, 2]. More recent analytical and experimental investigations have quantified the oil-film stiffness and damping in line or point contacts, linking film properties to vibration amplitude and frequency response [9, 10]. These works confirm that oil-film stiffness and damping play a decisive role in the stability and dynamic response of lubricated systems. Analytical approaches, including the homotopy analysis method, have also been applied to squeeze-film flow problems involving non-Newtonian fluids and nanofluids under various thermal and magnetic conditions [19, 20], further demonstrating the versatility of thin-film lubrication frameworks beyond classical Newtonian assumptions. Despite these advances, most existing studies treat pressure as the primary simulation output [5, 11, 13], while in vibration modeling, the time-varying film thickness governs the dynamic response and stability of the system. Only a few investigations explicitly incorporate lubrication-induced stiffness and damping into vibration analysis frameworks [9, 10, 12]. Therefore, a simplified yet physically consistent model coupling the Reynolds equation with a vibration analysis module remains necessary to predict the dynamic response of the oil film-piston system under realistic operating conditions.

In this work, a finite difference solver is developed to compute the oil film thickness in a hydraulic piston pump, including contact correction effects to prevent non-physical film collapse. Although analytical solutions to the Reynolds equation exist for simplified geometries, the distribution plate considered here involves a non-uniform annular film with spatially varying pressure boundary conditions corresponding to the alternating high and low pressure arcs of the piston orifices; a finite-difference approach is therefore adopted to handle these conditions without geometric simplification. Based on the resulting hydrodynamic and contact forces, equivalent stiffness and damping coefficients of the lubricating film are estimated using analytical relations derived from classical squeeze-film lubrication theory. These coefficients are then integrated into a simplified single-degree-of-freedom vibration model to analyze the influence of lubrication-induced dynamic properties on the vibration response of the piston–distribution plate system. In this framework, pressure is not treated as a primary result, but rather as an intermediate variable required to update the oil film thickness and associated forces. The contribution of this work lies in providing a physically consistent coupling between lubrication modeling and vibration analysis, enabling a qualitative investigation of how oil-film stiffness and damping affect vibration regimes in hydraulic piston pumps. The proposed approach is intended as a preliminary modeling framework, highlighting key trends and limitations, rather than as a fully validated predictive tool.

2 Theoretical Model

2.1 Governing Reynolds Equation and Oil Film Thickness

The main computational basis for the distribution of the pressure field of the oil film gap is the Reynolds equation for fluid lubrication. The Reynolds equation is derived from the Navier-Stokes equation and the continuity equation under certain assumptions.

In this work, the form of the Reynolds equation in cylindrical coordinates is adopted:

$$\frac{1}{r}\frac{\partial}{\partial r}\left(r\frac{h^3}{12\mu}\frac{\partial p}{\partial r}\right)+\frac{1}{r^2}\frac{\partial}{\partial \theta}\left(\frac{h^3}{12\mu}\frac{\partial p}{\partial \theta}\right)=\frac{U}{2r}\frac{\partial h}{\partial \theta}+\frac{\partial h}{\partial t} \tag{1}$$

where p is the hydrodynamic pressure, h is the film thickness, μ the dynamic viscosity of the oil evaluated at the operating temperature of 40°C, and U the sliding velocity. The left-hand side terms represent the Poiseuille flow contributions in the radial and circumferential directions, governing the pressure-driven flow through the converging-diverging film gap; their magnitude is governed by the cubic film thickness $h^3/12\mu$, reflecting the strong sensitivity of lubrication capacity to film thickness [2, 8]. On the right-hand side, there is first the wedge term arising from the relative tangential sliding velocity U, which generates hydrodynamic pressure through the wedge effect [2, 8]. The last term $\partial h/\partial t$ is the squeeze-film term, which captures the transient pressure generation due to the normal approach velocity of the two surfaces [2, 8].

This formulation results from the standard thin-film lubrication assumptions, where the lubricant is considered Newtonian and incompressible, the film thickness h is much smaller than the piston radius, and inertial effects are negligible compared to viscous effects. Only the sliding velocity U between piston and cylinder and the squeeze-film term $\partial h/\partial t$ are retained as sources of hydrodynamic pressure generation, since the plate undergoes pure axial translation with no imposed tangential sliding velocity.

A more general form of the Reynolds equation exists, including additional terms, as well as more complex film deformation contributions. While this extended formulation is appropriate for journal bearings under rotation or systems with significant multidirectional flows, it introduces additional unknowns and computational complexity. Since the hydraulic piston pump considered here is primarily subjected to axial translation, without imposed radial or tangential velocities, these higher-order contributions can be neglected. Therefore, the simplified Reynolds equation is not only consistent with the physical operating conditions of the piston–cylinder system, but also well-suited for numerical solution with the finite difference method. It provides the necessary accuracy to evaluate the pressure distribution and to capture the coupled evolution of oil film thickness and vibration response, while avoiding unnecessary mathematical complexity. The boundary conditions applied to Eq. (1) are of Dirichlet type: the discharge pressure is prescribed along the high-pressure arc and the suction pressure along the low pressure arc. Periodic conditions are imposed in the circumferential direction. A full-film, no-cavitation assumption is retained, consistent with the operating pressure range considered, in which the minimum pressure remains above zero. The local oil film thickness between the distribution plate and the cylinder block is defined as:

$$h(r,\theta) = H_c - r\cos(\theta)\tan(\alpha) - r\sin(\theta)\tan(\beta) \quad (2)$$

where h is the instantaneous film thickness. This expression models the local gap between the stationary distribution plate and the rotating cylinder block, where the plate undergoes a small angular tilt described by angles α and β about the x and y axes, respectively. The terms $-r\cos(\theta)\tan(\alpha)$ and $-r\sin(\theta)\tan(\beta)$ represent the linear variation of the gap in the radial direction due to the tilt of the plate, which increases with radial distance r from the center. This formulation is standard in the lubrication modeling of axial piston pump valve plates [8, 11].

When $h(r,\theta)$ locally approaches a critical threshold h_{crit}, a corrective contact force is introduced to prevent non-physical negative film thickness:

$$h(r,\theta) \geq h_{\text{crit}} \quad (3)$$

with h_{crit} representing the contact limit. This mechanism captures the transition from hydrodynamic to mixed lubrication regimes, where partial solid contact occurs.

2.2 Finite Difference Method

For the numerical solution of the Reynolds equation, the finite difference method (FDM) is adopted because of its simplicity, stability, and suitability for structured cylindrical domains. The lubrication gap between piston and cylinder is naturally expressed in radial and circumferential coordinates, allowing the film to be discretized on a uniform two-dimensional grid. The FDM scheme ensures both accuracy and numerical stability through central-difference approximations of the pressure gradients and a consistent treatment of the film thickness derivatives. The discretized Reynolds equation forms a sparse linear system of the form:

$$A \times p = b \quad (4)$$

where the matrix A depends on local film geometry $h(r,\theta)$ and lubricant viscosity μ. An iterative relaxation procedure is applied at each time step until the residual between successive pressure fields falls below a predefined convergence tolerance (typically 10^{-6}). The choice of FDM is therefore motivated by its compatibility with the cylindrical geometry of the hydraulic piston pump, the reduced computational cost for time-dependent simulations, and its ability to capture pressure gradients and oil film thickness variations with sufficient accuracy for vibration analysis. It offers sufficient resolution to capture local pressure gradients and film thickness variations that directly affect stiffness, damping, and vibration response.

2.3 Dynamic Coefficients: Analytical Estimation of Stiffness K and Damping C

In a hydraulic piston pump, the oil film separating the rotating and stationary components behaves as a dynamic elastic-viscous layer. Its mechanical behaviour can be idealized as a spring-damper system, where the stiffness K quantifies the resistance of the film to deformation, and the damping coefficient C represents the viscous energy dissipation during oscillatory motion. These coefficients govern the transmission of forces and the stability of the lubrication interface. In this work, these coefficients are estimated analytically from the mean pressure and film thickness obtained from the Reynolds solver. Assuming a circular equivalent contact region of effective radius R_{eff}, the hydrodynamic stiffness and damping coefficients are derived from the following closed-form relations:

$$K = \frac{3\pi R_{\text{eff}}^4 p_{\text{mean}}}{2h_{\text{mean}}^3} \quad (5)$$

$$C = \frac{3\pi R_{\text{eff}}^4 \mu}{2h_{\text{mean}}^3} \quad (6)$$

where p_{mean} is the mean pressure, h_{mean} is the oil film mean thickness, and R_{eff} represents the effective film radius between the outer and inner sealing bands. These equations are derived from the analytical solution of squeeze-film theory, assuming laminar flow, negligible inertia, and small harmonic perturbations of the film thickness. The analytical expressions for stiffness and damping are derived from classical squeeze-film lubrication theory [8]. They reveal the cubic inverse dependence of both stiffness and damping on the film thickness, a fundamental characteristic of hydrodynamic lubrication behaviour. However, these idealized relations tend to over-predict real stiffness and damping, since they assume a fully loaded bearing area, uniform pressure over the contact surface, and negligible compliance of the structural components. It is well documented that such idealized formulations tend to overestimate effective dynamic coefficients due to assumptions of uniform pressure distribution and rigid surfaces [2]. A calibration factor of 10^{-4} is applied to align the theoretical predictions with experimental values reported in the literature for lubricated contacts in rotating machinery, where typical oil-film stiffness and damping values range approximately from 10^6 to 10^8 N/m and 10^{-3} to 10^{-1} N·s·m^{-1} respectively [9, 10]. The factor 10^{-4} was selected so that the baseline stiffness lies inside the range of oil film dynamic coefficients reported for lubricated interfaces in the literature [8–10]. The analytical formulation offers a simple yet physically meaningful way to capture the viscoelastic behaviour of the oil film, enabling investigation of how the operating parameters — viscosity, pressure, speed, and inclination angle — affect the equivalent stiffness and damping coefficients.

2.4 Vibration Model of the Oil Film System

Once the equivalent stiffness K and damping coefficient C of the oil film have been obtained from the analytical model (Section 2.3), a simplified single-degree-of-freedom (SDOF) dynamic system is constructed to predict the vibration behaviour of the distribution plate–piston assembly. The motion of the equivalent mass M is governed by the following differential equation:

$$M\ddot{x}(t) + C\dot{x}(t) + Kx(t) = F(t) \quad (7)$$

where $x(t)$ represents the instantaneous displacement of the distribution plate, and $F(t)$ denotes an external excitation or imbalance force acting on the system. For a harmonic excitation $F(t) = F_0 \sin(\omega t)$, the steady-state vibration amplitude is obtained analytically as:

$$|X(\omega)| = \frac{1}{\sqrt{(K - M\omega^2)^2 + (C\omega)^2}} \quad (8)$$

This expression defines the frequency response function (FRF) of the lubricated interface, where the amplitude $|X(\omega)|$ represents the steady-state displacement magnitude as a function of excitation angular frequency ω. The resonance peak occurs near the natural angular frequency, indicating the dynamic stiffness of the system. For free vibration, $F(t) = 0$, the displacement response is expressed as:

$$x(t) = X_0 e^{-\zeta\omega_n t} \cos(\omega_d t) \quad (9)$$

where the damped natural angular frequency is given by:

$$\omega_d = \omega_n \sqrt{1 - \zeta^2} \quad (10)$$

and the parameters are:

$$\omega_n = \sqrt{\frac{K}{M}} \quad (11)$$

$$f_n = \frac{\omega_n}{2\pi} \quad (12)$$

$$\zeta = \frac{C}{2\sqrt{KM}} \quad (13)$$

where ω_n and f_n are the undamped natural angular and cyclic frequencies, respectively, and ζ is the dimensionless damping ratio. Since the damping coefficient C is relatively small, the system exhibits a nearly undamped oscillatory motion, characteristic of high stiffness and low energy dissipation in the lubricating film. The analytical vibration model provides direct access to two key quantities — the natural frequency f_n and the damping ratio ζ — which are essential indicators of the system's stability.

3 Numerical Solver and Simulation Results

3.1 Computational Setup

To numerically evaluate the oil film behaviour in the distribution plate of a hydraulic piston pump, a dedicated solver is developed. This solver integrates the Reynolds Equation with oil film thickness correction and pressure boundary conditions under various operating parameters. Table 1 presents the list of parameters and variables used in the simulation:

A schematic showing the computational process from initialization to convergence is also depicted in Figure 1.

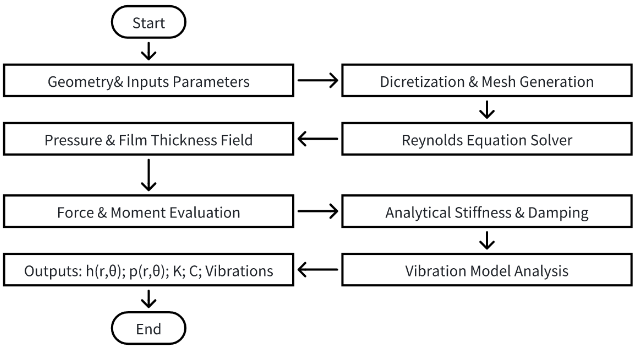

Figure 1. Flow chart of the Numerical Model.

The coupled Reynolds and elasticity equations were solved using FDM on a structured mesh with N_r = 100 radial and N_θ = 360 circumferential nodes. Convergence was achieved when both the total force and moment residuals were below the defined tolerance.

3.2 Oil Film Thickness and Pressure Distribution

This subsection analyzes the hydrodynamic field obtained from the Reynolds solver, focusing on the oil film thickness and pressure distribution across the sealing bands.

Figures 2 and 3 illustrate the reference case corresponding to a discharge pressure of $p_p = 21.5\,\text{MPa}$, rotation speed $\omega = 4000\,\text{rpm}$, inclination angle $\gamma = 14°$, and oil viscosity $\mu = 7.7 \times 10^{-4}\,\text{Pa·s}$. The pressure distribution is obtained from the finite-difference solution of Eq. (1), and the oil film thickness distribution is computed from Eq. (2). Under these conditions, the maximum hydrodynamic pressure reaches $21.5\,\text{MPa}$ near the high-pressure crescent region, while the minimum pressure stabilizes at $0.2\,\text{MPa}$ at the suction side. The pressure field exhibits a typical hydrodynamic wedge pattern, with a gradual pressure rise along the converging region and a sharp drop across the cavitation boundary. The corresponding oil film thickness varies between $h_{\text{min}} = 5.66 \times 10^{-4}\,\text{m}$ and $h_{\text{max}} = 5.74 \times 10^{-4}\,\text{m}$, with a mean value $h_{\text{mean}} = 5.70 \times 10^{-4}\,\text{m}$, confirming that the interface operates entirely within the full-film lubrication regime.

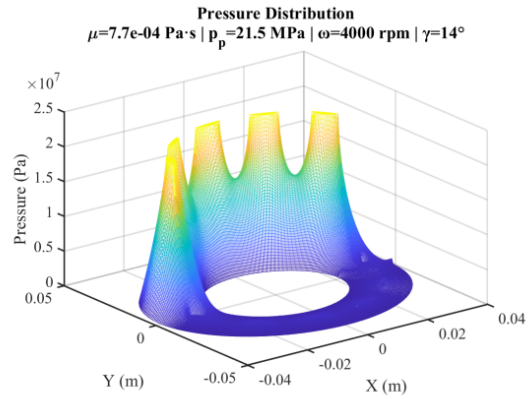

Figure 2. Pressure Distribution obtained from the finite-difference solution of Eq. (1) for Simulation 1.

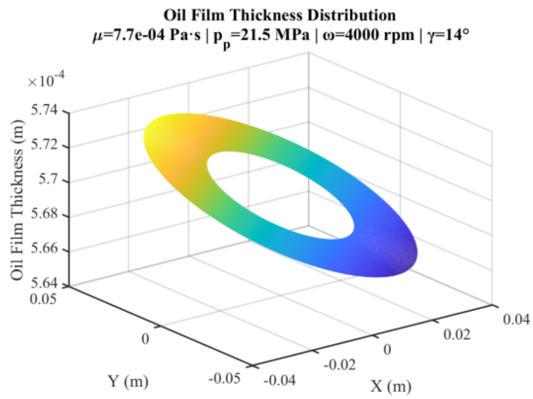

Figure 3. Oil Film Thickness Distribution computed from Eq. (2) for Simulation 1.

To assess the impact of operating parameters, additional simulations were performed by varying discharge pressure, viscosity, rotational speed, and swash-plate inclination angle. Results are shown in Figures 4, 5, 6 and 7.

Figures 4, 5, 6, 7 and Table 2 show that the mean pressure p_{mean} increases proportionally with the discharge pressure p_p, validating the hydraulic consistency of the model. The mean film thickness h_{mean} remains constant across all simulations, with $h_{\text{mean}} \approx 5.70 \times 10^{-4}\,\text{m}$. These results indicate that, within the limited range of operating conditions investigated, the mean film thickness appears to be

Table 1. Parameters and variables description.

Category	Parameter Description	Symbol	Baseline Case Value	Unit
Geometry	Radial coordinate	r	-	m
	Circumferential coordinate	θ	-	rad
	Outer and Inner sealing band radius	R_1, R_2	$38.9 \times 10^{-3}, 31.5 \times 10^{-3}$	m
	Outer and Inner inner-seal radius	R_3, R_4	$28.5 \times 10^{-3}, 21 \times 10^{-3}$	m
	Piston and piston distribution radius	R_p, R_s	$7.0 \times 10^{-3}, 36.5 \times 10^{-3}$	m
	Length Distribution plate	L_{dis}	78.8×10^{-3}	m
	Number of pistons	z	11	-
	Angular pitch	$a = 2\pi/z$	0.5712	rad
	Orifice opening angle	α_0	$35.4 \times \pi/180 = 0.618$	rad
Inclination	Initial central film	H_c	4.0×10^{-5}	m
	Swash-plate inclination angle	γ	$14° = 0.2443$	rad
Fluid & Contact	Dynamic viscosity	μ	7.7×10^{-4}	Pa·s
	Ambient, suction and discharge pressures	p_{oil}, p_x, p_p	$0.2 \times 10^6, 0.5 \times 10^6, 21.5 \times 10^6$	Pa
	Critical film thickness	h_{crit}	1.9×10^{-6}	m
Kinematics	Rotational speed	ω	$4000\,\text{rpm} = 418.9$	rad·s^{-1}
	Piston force	F_{press}	Computed	N
Numerical Solver	Circumferential and radial nodes	N_θ, N_r	360, 100	-
	Mesh spacing	$\Delta\theta, \Delta r$	$1.745 \times 10^{-2}, 1.79 \times 10^{-4}$	rad, m
	Pressure solver tolerance	ϵ_p	10^{-6}	-
Analytical Dynamic Coef.	Mean pressure and film thickness	$p_{\text{mean}}, h_{\text{mean}}$	-	Pa, m
	Effective equivalent radius	R_{eff}	30×10^{-3}	m
	Analytical stiffness	K	-	N·m^{-1}
	Analytical damping	C	-	N·s·m^{-1}
	Calibration factor	C_{factor}	10^{-4}	-
Vibration Model	Moving mass	M_{eq}	0.0116	kg
	Natural angular frequency	ω_n	-	rad·s^{-1}
	Natural frequency	f_n	-	Hz
	Damping ratio	ζ	-	-
	External excitation	$F(t)$	-	N
Outputs	Pressure field	$p(r, \theta)$	-	Pa
	Oil film thickness field	$h(r, \theta)$	-	m
	Oil-film force and moment	$F_{\text{oil}}, M_{\text{oil}}$	-	N, N·m
	Contact force	F_c	-	N
	Stiffness and Damping	K, C	-	N·m^{-1}, N·s·m^{-1}
	Vibration response	$x(t)$	-	m

Table 2. Key results for the oil film thickness and the pressure distributions.

Simulation	μ (Pa·s)	p_p (MPa)	ω (rpm)	γ (°)	p_{mean} (MPa)	h_{min} (m)	h_{max} (m)
1	7.7×10^{-4}	21.5	4000	14	4.72	5.66×10^{-4}	5.74×10^{-4}
2	5.0×10^{-4}	10	2000	10	2.39	5.68×10^{-4}	5.71×10^{-4}
3	1.0×10^{-3}	30	6000	18	6.44	5.64×10^{-4}	5.75×10^{-4}

primarily influenced by geometric configuration and contact correction mechanisms.

From a physical standpoint, this weak dependence of h_{mean} on operating conditions can be explained by several factors. First, the contact correction mechanism imposes a minimum admissible gap h_{crit} that prevents non-physical interpenetration; the solver thus converges toward an equilibrium thickness constrained by this limit. Second, the inclination angle γ and initial central film height H_c geometrically define a baseline profile that dominates the final solution. Third, the model operates in a quasi-static regime, where transient squeeze effects are negligible compared with steady hydrodynamic pressure generation.

As a result, while the local pressure distribution adapts sensitively to load and viscosity, the overall mean film thickness remains locked near its geometric equilibrium value.

Overall, the film thickness variation across all cases confirms that the solver maintains a stable full-film lubrication regime, ensuring the reliability of subsequent stiffness and damping coefficient

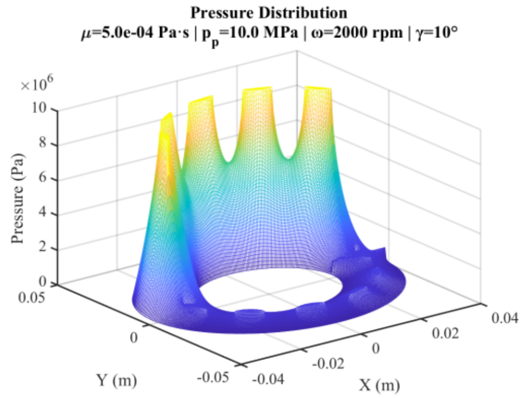

Figure 4. Pressure Distribution obtained from the finite-difference solution of Eq. (1) for Simulation 2.

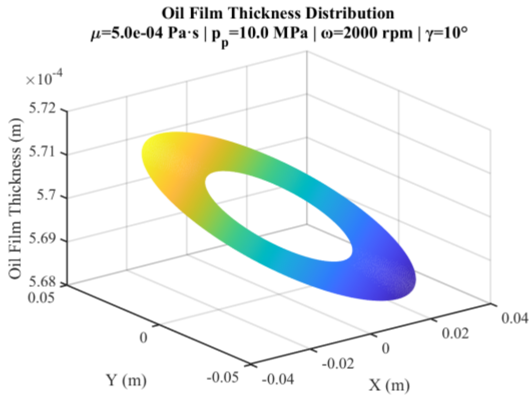

Figure 5. Oil Film Thickness Distribution computed from Eq. (2) for Simulation 2.

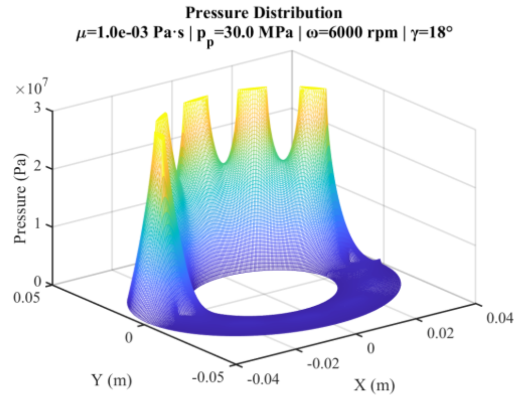

Figure 6. Pressure Distribution obtained from the finite-difference solution of Eq. (1) for Simulation 3.

estimations.

The present study does not include a formal numerical validation against a published benchmark. However, indirect consistency checks support the reliability of the solver: the mean pressure p_{mean} scales proportionally with discharge pressure across all three simulations (Table 2), confirming hydraulic consistency; the calibrated stiffness values fall within

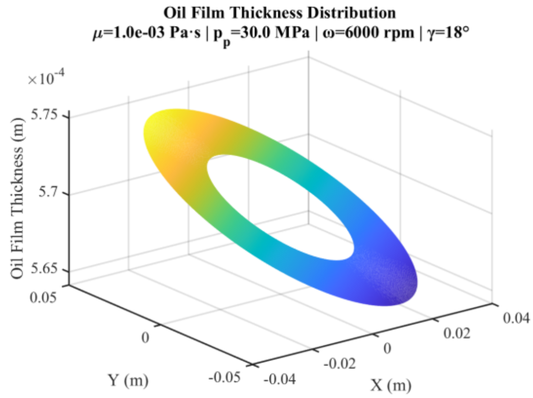

Figure 7. Oil Film Thickness Distribution computed from Eq. (2) for Simulation 3.

the range reported for lubricated contacts in rotating machinery [9, 10]; the natural frequencies obtained are consistent with typical piston pump vibration ranges reported in [3, 4]. Full experimental validation is identified as a necessary direction for future work.

3.3 Extraction of Dynamic Coefficients: Stiffness K and Damping C

This subsection evaluates the dynamic characteristics of the lubricating oil film by estimating its equivalent stiffness and damping coefficients through both analytical and force-based approaches. These coefficients characterize the elastic and viscous behaviour of the film under small perturbations, directly linking lubrication dynamics to the vibration response of the piston–plate interface.

The force-based approach computes coefficients directly from the pressure-induced force amplitude and film thickness variation.

As shown in Table 3, the analytical stiffness K_{cal} does not exhibit a simple monotonic trend with discharge pressure. The highest value occurs at the lowest pressure condition (Simulation 2: 9.97×10^7 N·m^{-1} at 10 MPa), while the baseline and high-pressure cases yield 1.97×10^7 and 2.69×10^7 N·m^{-1}, respectively. This non-monotonic behaviour suggests that stiffness is influenced by the combined effects of pressure, viscosity, rotational speed, and swash-plate inclination angle rather than pressure alone.

The damping coefficients show better consistency, with force-based values clustering around 11 N·s·m^{-1} across all operating conditions, while analytical values range from 2.09×10^{-3} N·s·m^{-1} to 4.17×10^{-4} N·s·m^{-1}.

Physically, this difference arises from several factors. First, the analytical expressions assume a fully

Table 3. Dynamic coefficients extracted for the three operating conditions.

Simulation	K_{cal}	C_{cal}	K_{force}	C_{force}
1	1.97×10^{7}	3.21×10^{-4}	4.36×10^{9}	1.13×10^{1}
2	9.97×10^{7}	2.09×10^{-4}	4.22×10^{9}	1.10×10^{1}
3	2.69×10^{7}	4.17×10^{-4}	4.43×10^{9}	1.14×10^{1}

developed hydrodynamic film with uniform pressure over the entire contact area, while the force-based estimation inherently accounts for non-uniform pressure distribution and localized deformation. Second, the contact correction mechanism used in the numerical solver restricts the minimum admissible film thickness, effectively increasing the apparent stiffness of the system. Third, the pressure integration in the force-based method tends to overestimate the effective load-bearing area when expressed as $A \times p = b$, leading to higher values of K and C.

3.4 Vibration Analysis

The dynamic response of the piston-distribution plate system was evaluated using the equivalent stiffness and damping coefficients.

The film behaviour is modeled as a single degree-of-freedom oscillator with M_{eq} as equivalent mass.

Table 4 demonstrates physically consistent behaviour: natural frequencies increase with operating pressure, ranging from 4.67 kHz to 7.66 kHz. The consistent near-zero damping ratios ($\zeta \approx 0$) across all conditions confirm that the oil film's limited damping capacity is an inherent characteristic rather than an operating-condition dependent phenomenon.

The calibrated analytical approach exhibits distinct resonance peaks that shift with operating parameters, as depicted in Figure 8.

The force-based parameters yield fundamentally different behaviour, with no discernible resonance peaks within the 0-20 kHz range. This flat response profile indicates that the excessively high stiffness values dominate the system dynamics, effectively suppressing vibrational motion.

The free vibration analysis is depicted in Figure 9, and reveals critically different damping characteristics between the two methods.

The analytical solution shows persistent oscillations with negligible amplitude decay over 10 ms, consistent with the near-zero damping ratios calculated for the

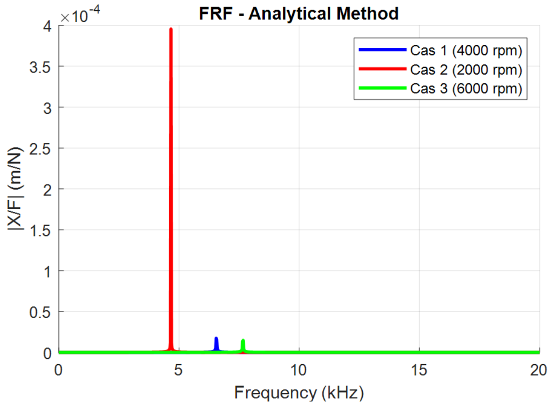

Figure 8. Frequency Response Function for the three Cases of the Analytical Method only.

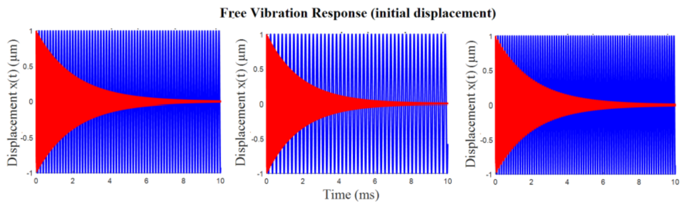

Figure 9. Free Vibration Response for case 1, 2 and 3 respectively.

three cases. The force-based parameters produce immediate decay without oscillations. This quick dissipation contradicts practical observations of piston pump vibrations and underscores the physical inconsistency of the force-based stiffness estimation.

4 Physical Interpretation

The dramatic divergence between the two estimation methods provides critical insights for pump design. First, the oil film stiffness dominates dynamics. The analytical results confirm that the oil film provides substantial elastic support, with natural frequencies from 4.67 kHz to 7.66 kHz falling within typical ranges for piston pump vibrations. This stiffness is essential for maintaining structural integrity but necessitates complementary damping mechanisms.

Second, the persistent oscillations in free vibration response and sharp resonance peaks in forced response demonstrate that the oil film's viscous dissipation is insufficient for vibration control. The calculated

Table 4. Vibration parameters for the three operating conditions.

Simulation	f_n (kHz) analytical	f_n (kHz) force-based	ζ analytical	ζ force-based
1	6.56	97.5	0	0.001
2	4.67	96.0	0	0.001
3	7.66	98.4	0	0.001

damping ratios ($\zeta \leq 0.001$) are orders of magnitude below the critical damping threshold ($\zeta = 1$).

Third, regarding force-based method limitations, while the force-based damping coefficients ($C \approx 11\,\mathrm{N{\cdot}s{\cdot}m^{-1}}$) fall within plausible ranges, the associated stiffness values are physically inconsistent with measured pump dynamics.

The vibration analysis conclusively demonstrates that while the oil film provides excellent elastic support for the piston-distribution plate interface, its intrinsic damping capacity is fundamentally inadequate for vibration suppression. This finding emphasizes the necessity of integrated damping strategies in the design of high-performance, low-vibration hydraulic piston pumps.

In practical hydraulic piston pumps, measured vibration spectra typically exhibit distinct resonance peaks and sustained oscillations, rather than the flat response predicted by excessively high stiffness values [2, 4, 6].

5 Conclusion

This research successfully developed and applied an integrated model that couples fluid dynamics with structural vibration to analyze the impact of the lubricating oil film on the dynamic behaviour of a hydraulic piston pump. The key findings are summarized as follows.

First, the study successfully quantified oil film dynamics. The Reynolds equation, solved via the finite difference method (FDM), effectively predicted the oil film pressure and thickness distributions under varying operational parameters. The results indicated that the mean film thickness remained stable across simulations, governed primarily by geometric configuration and the contact correction mechanism, confirming operation within a stable full-film lubrication regime.

Second, a comparative analysis of stiffness and damping was conducted. The dynamic coefficients were extracted using both analytical and force-based approaches. The calibrated analytical method provided physically consistent stiffness values that vary with operating conditions. In contrast, the force-based method yielded stiffness estimates orders of magnitude higher, leading to unrealistic vibration response predictions, as shown by the absence of resonance peaks in the frequency response function.

Third, the analysis revealed the dual role of the oil film in vibrations. The vibration analysis clearly delineates the dual role of the oil film: it provides substantial elastic support, resulting in high natural frequencies (4.67–7.66 kHz) essential for structural integrity; however, its damping capacity is negligible (damping ratio $\zeta \approx 0$), as evidenced by persistent oscillations in free vibration response and sharp resonance peaks in forced response, proving its inadequacy for vibration suppression.

This study could be further pursued by implementing a more sophisticated time-domain integration scheme, such as the Newmark method, for the vibration analysis. This would allow for the investigation of transient dynamic responses and non-linear phenomena under complex loading conditions. Furthermore, experimental validation of the simulated dynamic coefficients and vibration response is crucial for further model refinement.

The present study does not provide experimental validation. The results are intended to highlight qualitative trends and physical consistency with established lubrication and vibration literature. Experimental validation and advanced coupled fluid-structure models will be addressed in future work.

From the perspective of carbon neutrality, the findings of this study carry relevant implications for sustainable engineering. Hydraulic piston pumps are integral to energy-intensive industrial and aerospace systems, and any reduction of mechanical losses at lubricated interfaces translates directly into lower energy consumption and reduced carbon footprint over the equipment lifecycle. The identification of the oil film's inadequate damping capacity as a critical design limitation opens concrete pathways for improvement: incorporating active or passive supplementary damping mechanisms, such as viscoelastic materials, magnetorheological fluids, or optimized valve timing strategies, can reduce vibration-induced wear and extend component life, thereby decreasing the frequency of replacement and the associated manufacturing emissions. Moreover, the simulation framework developed here can be extended to guide the selection of bio-based or synthetic low-viscosity lubricants with favorable environmental profiles, which simultaneously reduce fluid friction losses and minimize ecological impact. Future work integrating this model with lifecycle carbon assessment tools could provide quantitative guidance for the design of hydraulic systems aligned with net-zero targets in the aerospace, automotive, and industrial sectors.

Data Availability Statement

Data will be made available on request.

Funding

This work was supported without any funding.

Conflicts of Interest

The authors declare no conflicts of interest.

AI Use Statement

The authors declare that no generative AI was used in the preparation of this manuscript.

Ethical Approval and Consent to Participate

Not applicable.

References

[1] Ivantysyn, J., & Ivantysynova, M. (2001). *Hydrostatic Pumps and Motors: Principles, Design, Performance, Modelling, Analysis, Control and Testing*. Fluid Power Net Publications.

[2] Manring, N. (2013). *Fluid power pumps and motors: analysis, design, and control* (pp. 107-116). New York, NY, USA: McGraw-Hill Education. https://www.mheducation.com/highered/mhp/product/fluid-power-pumps-motors-analysis-design-control.html

[3] Milind, T. R., & Mitra, M. (2016). A study on the dynamics and vibration behavior of an axial piston pump using combined MBD/FE approach. *Procedia engineering, 144*, 452-460. [CrossRef]

[4] Wang, W. (2017). Vibration model and characteristic analysis of hydraulic piston pump. *Chemical Engineering Transactions, 59*, 61-66. [CrossRef]

[5] Ye, S., Zhang, J., Wang, X., Tang, H., & Zhang, Y. (2021). A theoretical dynamic model to study the vibration response characteristics of an axial piston pump. *Mechanical Systems and Signal Processing, 150*, 107237. [CrossRef]

[6] Ye, S., Zhang, J., Xu, B., Zhu, S., Xiang, J., & Tang, H. (2019). Theoretical investigation of the contributions of the excitation forces to the vibration of an axial piston pump. *Mechanical Systems and Signal Processing, 129*, 201-217. [CrossRef]

[7] Ying, P., Tang, H., Chen, L., Ren, Y., & Kumar, A. (2023). Dynamic modeling and vibration characteristics of multibody system in axial piston pump. *Alexandria Engineering Journal, 62*, 523-540. [CrossRef]

[8] Hamrock, B. J., Schmid, S. R., & Jacobson, B. O. (2004). *Fundamentals of fluid film lubrication*. CRC press. [CrossRef]

[9] Zhou, C., & Xiao, Z. (2018). Stiffness and damping models for the oil film in line contact elastohydrodynamic lubrication and applications in the gear drive. *Applied Mathematical Modelling, 61*, 634-649. [CrossRef]

[10] Zhang, Y., Liu, H., Zhu, C., Liu, M., & Song, C. (2016). Oil film stiffness and damping in an elastohydrodynamic lubrication line contact-vibration. *Journal of Mechanical Science and Technology, 30*(7), 3031-3039. [CrossRef]

[11] Wang, Z., Hu, S., Ji, H., Wang, Z., & Liu, X. (2018). Analysis of lubricating characteristics of valve plate pair of a piston pump. *Tribology International, 126*, 49-64. [CrossRef]

[12] Pelosi, M., & Ivantysynova, M. (2012). Heat Transfer and Thermal Elastic Deformation Analysis on the Piston/Cylinder Interface of Axial Piston Machines. *Journal of Tribology, 134*(4). [CrossRef]

[13] Yongling, F. U., Jiming, M. A., Jian, F. U., Qun, C. H. A. O., & Yan, W. A. N. G. (2021). Review of cylinder block/valve plate interface in axial piston pumps: Theoretical models, experimental investigations, and optimal design. *Chinese Journal of Aeronautics, 34*(1), 111-134. [CrossRef]

[14] Shengrong, G. U. O., Jinhua, C. H. E. N., Yueliang, L. U., Yan, W. A. N. G., & Hongkang, D. O. N. G. (2020). Hydraulic piston pump in civil aircraft: Current status, future directions and critical technologies. *Chinese Journal of Aeronautics, 33*(1), 16-30. [CrossRef]

[15] Peixin, G. A. O., Tao, Y. U., Jiao, W. A. N. G., & Jingyu, Z. H. A. I. (2021). Vibration analysis and control technologies of hydraulic pipeline system in aircraft: A review. *Chinese Journal of Aeronautics, 34*(4), 83-114. [CrossRef]

[16] Milind, T. R., & Mitra, M. (2016). A study on the

flexible multibody dynamic modeling of an axial piston pump considering housing flexibility. *Procedia Engineering*, *144*, 1234-1241. [CrossRef]

[17] Ye, S., Sun, Y., Zhang, J., Chen, J., Xu, B., Zhao, S., & Liu, H. (2025). A new coupled dynamic model to study the vibration and lubrication characteristics of slipper/swash-plate interface in an axial piston pump. *Proceedings of the Institution of Mechanical Engineers, Part J: Journal of Engineering Tribology*, *239*(8), 1026-1049. [CrossRef]

[18] Wu, H., Wang, T., Zhang, X., & Wang, D. (2026). Mechanical hydraulic coupling modeling and dynamic behavior analysis of piston pump. *Journal of the Brazilian Society of Mechanical Sciences and Engineering*, *48*(5), 340. [CrossRef]

[19] Xiao, Z., Li, Z., Shi, X., & Zhou, C. (2018). Oil film damping analysis in non-Newtonian transient thermal elastohydrodynamic lubrication for gear transmission. *Journal of Applied Mechanics*, *85*(3), 035001. [CrossRef]

[20] Tsuha, N. A. H., & Cavalca, K. L. (2020). Stiffness and damping of elastohydrodynamic line contact applied to cylindrical roller bearing dynamic model. *Journal of Sound and Vibration*, *481*, 115444. [CrossRef]

Avae Berger received the Bachelor's degree in Mechanical Engineering from Beihang University in 2023. She is currently pursuing a Master's degree in Systems Engineering at the Sino-French Engineering School, at Beihang University. Her research interests include hydraulic system dynamics, lubrication modeling, and vibration analysis in mechanical systems. She is dedicated to exploring advanced modeling and simulation techniques to improve the performance and reliability of hydraulic machinery. (Email: avae.berger@centralepekin.cn)

Jiming Ma received his Ph.D. degree and is currently an Associate Professor with the Sino-French Engineer School (ECPkn, École Centrale de Pékin), Beihang University (BUAA), Beijing, China. His research interests include fluid power transmission and control, industrial science and technology, reliability of hydraulic components, and multi-domain modeling. For more information, please visit http://ecpkn.buaa.edu.cn/english/. (E-mail: Jiming.ma@buaa.edu.cn)

Yunrui Zhang obtained a Bachelor's Degree in Applied Physics from Beihang University in 2024, possessing a solid foundation in physical theories and interdisciplinary insights into engineering disciplines. Currently, he is pursuing a Master's Degree at Beihang University. His core research interests include structural fault diagnosis, vibration and noise analysis. He places emphasis on exploring the practical application of relevant technologies, and committed to providing theoretical support and optimizing operational performance. (Email: violetmoon@buaa.edu.cn)

Xiangxiang Tian received the bachelor's degree in applied physics from Beijing University of Aeronautics and Astronautics in 2024. He is currently pursuing the master's degree in systems engineering at Beijing University of Aeronautics and Astronautics. His research areas include piston pump moving pair oil film calculation, high-speed piston pump dynamic balance, aircraft hydraulic system simulation, etc. (Email: sy2424140@buaa.edu.cn)